

Article

Environmental Impact Assessment and Classification of 48 V Plug-in Hybrids with Real-Driving Use Case Simulations

Tobias Frambach ^{1,2}, Ralf Kleisch ³, Ralf Liedtke ¹, Jochen Schwarzer ¹ and Egbert Figgemeier ^{2,4,*}

¹ Robert Bosch GmbH, Robert-Bosch-Straße 2, 71701 Schwieberdingen, Germany; tobias.frambach@de.bosch.com (T.F.); ralf.liedtke@de.bosch.com (R.L.); jochen.schwarzer@de.bosch.com (J.S.)

² Institute for Power Electronics and Electrical Drives (ISEA), RWTH Aachen University, Jägerstraße 17-19, 52066 Aachen, Germany

³ Institute of Automotive Engineering (IFS), University of Stuttgart, Pfaffenwaldring 12, 70569 Stuttgart, Germany; ralf.kleisch@ifs.uni-stuttgart.de

⁴ Helmholtz Institute Münster (HI MS), IEK-12, Forschungszentrum Jülich, Corrensstraße 46, 48149 Münster, Germany

* Correspondence: e.figgemeier@fz-juelich.de; Tel.: +49-241-809-7158

Abstract: Plug-in hybrid electric vehicles (PHEVs) are commonly operated with high-voltage (HV) components due to their higher power availability compared to 48 V-systems. On the contrary, HV-powertrain components are more expensive and require additional safety measures. Additionally, the HV system can only be repaired and maintained with special equipment and protective gear, which is not available in all workshops. PHEVs based on a 48 V-system level can offer a reasonable compromise between the greenhouse gas (GHG) emission-saving potential and cost-effectiveness in small- and medium-sized electrified vehicles. In our study, the lifecycle emissions of the proposed 48 V PHEV system were compared to a conventional vehicle, 48 V HEV, and HV PHEV for individual driving use cases. To ensure a holistic evaluation, the analysis was based on measured real-driving cycles including Global Position System (GPS) map-matched slope profiles for a parallel hybrid. Optimal PHEV battery capacities were derived for the individual driving use cases. The analysis was based on lifecycle emissions for 2020 and 2030 in Europe. The impact analysis revealed that 48 V PHEVs can significantly reduce GHG emissions compared to vehicles with no charging opportunity for all use cases. Furthermore, the findings were verified for two vehicle segments and two energy mix scenarios. The 48 V PHEVs can therefore complement existing powertrain portfolios and contribute to reaching future GHG emission targets.

Keywords: hybrid electric vehicle (HEV); plug-in hybrid electric vehicle (PHEV); 48 V; battery sizing; real-driving simulation; life cycle analysis; greenhouse gas (GHG) emissions



Citation: Frambach, T.; Kleisch, R.; Liedtke, R.; Schwarzer, J.; Figgemeier, E. Environmental Impact Assessment and Classification of 48 V Plug-in Hybrids with Real-Driving Use Case Simulations. *Energies* **2022**, *15*, 2403. <https://doi.org/10.3390/en15072403>

Academic Editors:

Pablo García-Triviño and Carlos Andrés García-Vázquez

Received: 25 February 2022

Accepted: 22 March 2022

Published: 24 March 2022

Publisher's Note: MDPI stays neutral with regard to jurisdictional claims in published maps and institutional affiliations.



Copyright: © 2022 by the authors. Licensee MDPI, Basel, Switzerland. This article is an open access article distributed under the terms and conditions of the Creative Commons Attribution (CC BY) license (<https://creativecommons.org/licenses/by/4.0/>).

1. Introduction

One quarter of the greenhouse gas (GHG) emissions in Europe originates from the transport sector [1]. One of today's main targets for the automotive industry is therefore a reduction of the environmental impact of vehicles. The electrification of the powertrain is a widely accepted method to reduce the amount of GHG emissions and can be scaled on different levels [2]. It was shown that 48 V hybrid electric vehicles (HEVs) offer a good compromise between additional investment costs and fuel-saving potentials [3]. However, to substitute more fossil fuel with electric energy, high voltage (HV) systems are necessary, which can recuperate more energy due to their lower current [4,5]. Plug-in hybrid electric vehicles (PHEVs) and battery electric vehicles (BEVs) utilize an external charge plug to use electrical grid energy and increase the electric driving share. Fuel cell vehicles are operated similarly to HEVs or PHEVs and allow the substitution of fossil fuel with hydrogen, which can reduce the CO₂ emissions further if the hydrogen is based on renewable energy sources.

Modelling approaches for those systems and different control studies have been reviewed in [6–8].

Especially for subcompact class vehicles, the additional costs, weight increase, and HV safety measures make the market introduction challenging for vehicles with high degrees of electrification [9]. It was shown that the power limitations of 48 V machines can be increased to over 30 kW, which already covers a large share of driving operating points [10]. Since the voltage level is set by safety regulations, the power is limited by the increasing current, which results in larger wire diameters, cooling efforts, and costs. Nevertheless, the power level is sufficient to propel the vehicle for inner-city mobility in pure electric mode and cover most recuperation situations [11].

In [12], several 48 V parallel hybrid topologies were analyzed in different driving cycles. Electric powers of up to 20 kW reduced the fuel consumption with a higher impact, whereas a further increase towards 30 kW decreased the overall system efficiency. The optimal battery capacity varied for the different simulated topologies and electric machine sizes. The largest reduction potential could be achieved in urban areas due to the higher share of launch and brake events. The largest reduction potential was achieved with topologies, where the electric engine is placed between the transmission and wheels in combination with a belt-integrated starter generator. The authors of [13] focused on the machine design during the system-level optimization process and considered the changes of the machine characteristics during the sizing process. Similarly, most of the fuel reduction potential could be gained with 20–25 kW mechanical power of the electric machine. The transfer to a 48 V PHEV is presented in [14] for a compact class vehicle. The peak power requirements were found to be between 25 and 30 kW at wheel level in the urban part of the WLTC. Even with a few occasions of higher power requirements in real-drive emission (RDE) testing, a 30 kW PHEV system reduced the CO₂ emissions in a WLTC as well as an RDE cycle significantly.

Especially for PHEVs, the optimal battery dimensioning is crucial due to the high battery costs and weight increase. At the same time, the capacity needs to be high enough to ensure a suitable electric range in real-life applications. Song et al. showed a component optimization of a hybrid energy storage system utilizing batteries and supercapacitors for a series-parallel PHEV bus, where the overall operational costs could be decreased [15]. The powertrain sizing process is often coupled with energy management strategy (EMS) optimization, as the two domains influence each other. This has been reviewed in [8,16]. Mahmoodi et al. investigated a simultaneous optimization of the system components and the EMS for a parallel PHEV [17]. A further reduction of the fuel consumption, emissions, and operating costs could be achieved compared to an individual optimization of the components and EMS. Including energy storage aging in the co-optimization process was studied for battery-only [18] and hybrid energy storage systems [19]. Furthermore, the drive cycle selection has a large influence on the optimal system layouts, so recent studies try to incorporate the cycle distribution and uncertainty in the optimization process [20,21] or improve the overall efficiency with predictive information [22]. In the latter study, it was possible to reduce the energy consumption by 3.7% if the Adaptive Equivalent Consumption Minimization Strategy (A-ECMS) was supported by speed-predictive information based on historical driving data.

In contrast to the previous studies, which focus on tank-to-wheel emissions, several published life cycle assessments (LCA) include the well-to-tank, production, and end-of-life emissions. Especially for PHEVs, the GHG-saving potential depends on the real-world driving cycles and charging habits. Nevertheless, the first PHEV generations reduced life-cycle GHG emissions according to an evaluation of empirical online fuel consumption databases [23], despite a large discrepancy towards test-cycle consumptions [24]. The authors emphasized the need for PHEVs with larger electric ranges, frequent battery charging events, and consideration of the electricity production in drivetrain comparisons. The importance of the electricity mix for different regions was studied in [25], where different driving patterns and electric energy mixes across the United States has led to

different optimal degrees of electrification. In cases of states with a carbon-intensive electricity mix, HEVs even showed lower life cycle GHG emissions compared to PHEVs and BEVs. However, on a national level, the largest GHG reduction potential was achieved with a PHEV. Despite the focus on the United States and high battery production emissions in the past, the analysis demonstrates the importance of renewable energies for the mobility sector. The authors in [26] underlined the LCA-saving potential of PHEVs, especially in combination with renewable fuels, which can be an additional measure to reduce greenhouse gases.

Extending a 48 V hybrid to a PHEV with a larger battery and an external charge plug can be a cost-efficient fuel-saving technology, which shall be further investigated in this article on an LCA basis for the first time. To this aim, our study also includes the emissions during the production phase of the vehicle and the well-to-tank emissions. Unlike previous studies, we conduct an LCA of a 48 V PHEV and compare it to results for a conventional vehicle, 48 V HEV, and HV PHEV to classify the proposed system against broadly existing technologies. Measured year-round speed and slope profiles from different driving use cases ensure the applicability towards real-world driving. Furthermore, the outcome of two different EMSs is shown to evaluate the influence of possible strategy improvements. The results are evaluated for a 2020 and 2030 energy mix scenario and include a comparison to the emission targets of the European Union (EU). Finally, based on the simulation results, policy implications for PHEVs are discussed.

The paper is organized as follows: The overall system model is presented in Section 2. This includes the derivation of the selected driving use cases, the powertrain model, the investigated EMSs of the vehicles, and the underlying assumptions for the LCA. The results of the LCA are shown in Section 3, followed by a discussion in Section 4. Finally, a conclusion is given in Section 5.

2. Research Method

The working principle of the conducted LCA is shown in Figure 1. First, vehicle speed and Global Position System (GPS) measurements were collected for 104 different vehicles. Four typical driving use cases were selected out of this database afterwards. The year-round trips served as an input for the powertrain simulation layer. The results were calculated for two different vehicle segments, two EMSs, and systems with different degrees of hybridization. Finally, the operation emissions were added to the GHG emissions from the production and recycling of the vehicle and battery. The input and powertrain simulation layers are explained in the following subsections.

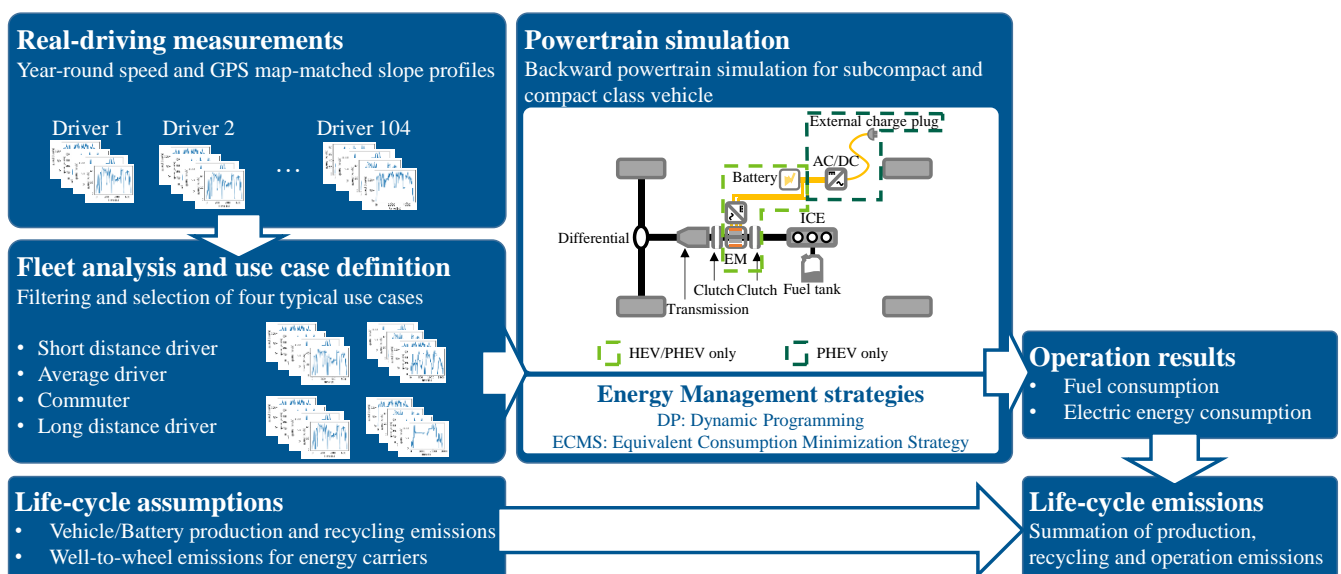


Figure 1. Schematic diagram of conducted LCA.

2.1. Fleet Analysis and Use Case Definition

The battery sizing problem for PHEVs is largely dependent on the use case [21]. It is important to consider the different trip distance shares during the usage of the vehicle for a realistic evaluation. Therefore, this analysis does not focus on individual cycles, and instead uses continuous trip data information.

The database used in this study consists of 104 vehicles operated in Germany for which we extracted the data until 30.03.2020 to eliminate influences of the pandemic. Four vehicle trip datasets were extracted from this subset, based on the following criteria:

- Short-distance driver, high share of trips less than 10 km;
- Average driver, annual mileage is close to German passenger car average of 13.602 km (2019) [27];
- Long-distance driver, high share of trips longer than 100 km;
- Commuter, prominent peak at a certain trip distance.

The key parameters of the selected drivers are shown in Table 1. The recorded timespan of more than 285 days ensures a robust extrapolation towards the annual distance. Individual routes on one driving day are merged for the simulation and defined as a trip in the following.

Table 1. Key parameters of selected use cases.

Use Case	Annual Distance (km)	Recorded Distance (km)	Recorded Timespan (Days)	Days with Usage (Days)	Usage Frequency (Routes/Day)
Short-distance driver	5314	4149	285	179	3.4
Average driver	12,862	10,078	286	171	4.1
Long-distance driver	31,930	31,930	365	287	4.2
Commuter	9410	8946	347	144	2.2

Furthermore, the driving style can influence the energy consumption of a vehicle, which was shown in [28]. To ensure the selection of realistic data, RDE testing criteria were used to evaluate the driving style [29]. During RDE testing, two boundary conditions need to be fulfilled, which are shown in for the four selected vehicles in comparison to the complete database. The 95 percentile of the product of vehicle speed and positive acceleration in (a) is used to identify high trip dynamics and is an upper limit, calculated as

$$va_{pos95} = va_{pos}\{95\} \quad (1)$$

where v is the vehicle speed and a_{pos} is the positive acceleration. The relative positive acceleration (RPA) in (b) is used as a lower boundary to filter out cycles which are too smooth, and is described as

$$RPA = \frac{\int va_{pos}dt}{d_i} \quad (2)$$

where d_i is the distance of a daily trip. The comparison of the selected drivers to the complete fleet data in Figure 2 shows that the drivers have an averaged driving style and stay within the limits for RDE testing for most daily trips, which ensures that no extremely aggressive or passive drivers are selected.

The energy consumption of PHEVs strongly depends on the share of electric-driven mileage compared to the total distances. The utility factor (UF) is a key parameter to determine this share and is used in many regulations worldwide [30]. The UF is dependent on the charge depleting (CD) range of a PHEV, and is calculated as

$$UF = \frac{\sum_{i=1}^n \min(d_i, R_{CD})}{\sum_{i=1}^n d_i} \quad (3)$$

where R_{CD} is the CD range and n is the total number of trips. Ideally, each driving day is assumed to start with a charged battery. The UF curves of the four drivers are shown in Figure 3 in comparison to the Worldwide Harmonized Light Vehicles Test Procedure

(WLTP) curve for Europe [29]. Except for the short-distance driver, the resulting curves are underneath the European WLTP UF curve. This is in accordance with other studies, where the real-life UF is lower, especially for company cars. The annual mileage and UF curves for the average driver and commuter fit to typical privately owned cars, whereas the long-distance driver curve matches a company car profile.

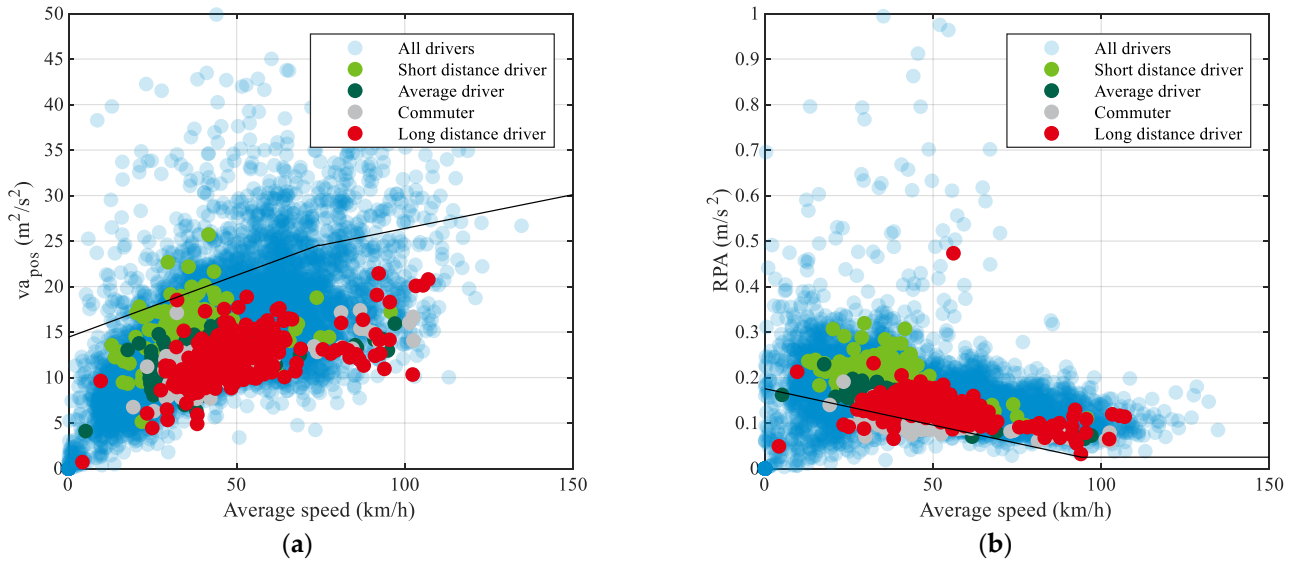


Figure 2. Comparison of (a) va_{pos} and (b) RPA of the selected drivers to the fleet data.

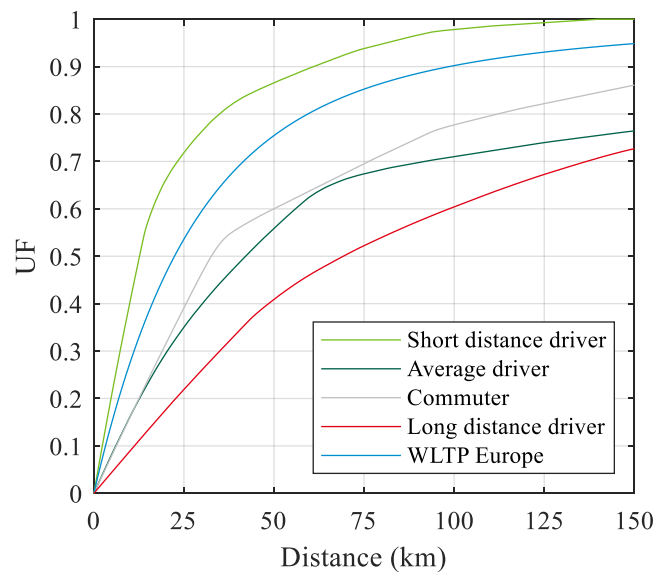


Figure 3. Utility factor curves for different use cases in comparison to the WLTP Europe curve.

2.2. Powertrain Simulation

The investigated systems in this study are shown in Figure 4. The conventional vehicle has no electrical driveline components, so the driving energy is obtained from the liquid fuel tank only. The HEV and PHEV systems are parallel hybrids, with an electric machine (EM) located between the ICE and transmission. The ICE can propel the vehicle together with the EM in a parallel hybrid mode, but can also be decoupled and turned off for pure electric driving. Both systems can harvest kinetic energy during regenerative braking and load shifting of the ICE. In contrast to the HEV, the PHEV systems have an external charge plug to charge the battery with additional electrical grid energy.

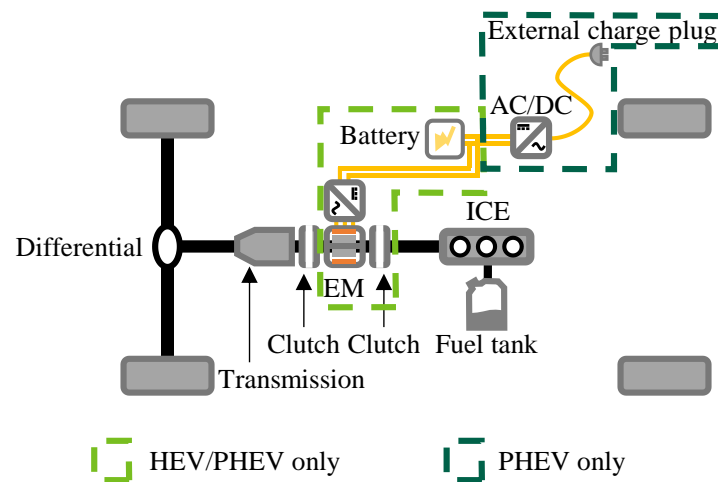


Figure 4. P2 parallel hybrid topology.

The main parameters of the two examined vehicles are shown in Table 2. In this study, the results for a subcompact class vehicle are compared to a compact class vehicle. The sales price of a subcompact class vehicle is typically lower, which makes the introduction of HV PHEVs in that vehicle segment difficult; 48 V PHEVs may reduce the cost barrier. Furthermore, the lower vehicle weight leads to lower required power demands. The occurrences of power demands exceeding the limits of 48 V systems are consequently lower, which allows larger driving shares in pure electric mode. Nevertheless, we also show the results for a compact class vehicle, because it addresses a larger market share [31].

Table 2. Vehicle parameters of the two investigated vehicle classes.

Property	Symbol	Subcompact Class	Compact Class
Vehicle base weight (kg)	m_0	1255	1565
Frontal area (m ²)	A	2.10	2.13
Air resistance coefficient	c_w	0.265	0.250
Rolling resistance coefficient	f_R	0.008	0.008
Tire radius (m)	r_{dyn}	0.3065	0.3065
Equivalent rotational inertia (kgm ²)	Θ	1.1	1.1
Gearbox mechanical efficiency	η_{Tra}	0.9	0.9

The powertrain equations are solved in a kinematic backward simulation in MATLAB. The mechanical power demand on wheel level is calculated as

$$P_{Whl} = (m_{veh} \frac{dv}{dt} \Theta + m_{veh} g f_R \cos \alpha + m_{veh} g \sin \alpha + 0.5 c_w A \rho_{Air} v^2) v \quad (4)$$

where m_{veh} is the vehicle mass, Θ is the equivalent rotational inertia, g is the gravitational acceleration, f_R is the tire-rolling resistance coefficient, α the climbing angle, c_w the air resistance coefficient, A the frontal area, and ρ_{Air} the air density. The vehicle mass m_{veh} is separated into three parts to address the component differences between the three hybrid systems and scale with increasing battery capacity:

$$m_{veh} = m_0 + m_{0,Edr} + \frac{E_{Bat}}{\rho_{Bat}} \quad (5)$$

where m_0 is the vehicle base weight, $m_{0,Edr}$ is the electric powertrain weight without the battery, E_{Bat} is the battery energy, and ρ_{Bat} is the battery gravimetric energy density.

The values for electric powertrain parameters are summarized in Table 3. Since 48 V PHEVs have a higher share of electric driving compared to HEVs, it is assumed that the weight increases due to enhanced cooling requirements and larger wire diameters. The

weight increase towards the HV PHEV is based on the higher EM power. The energy densities for the 48 V HEV and HV PHEV are derived from the average of current pack models on the market. The power-to-energy ratio of 48 V PHEVs is in the range of typical BEV applications, which allows the usage of cells with a higher energy density. If the fill factor of a PHEV battery pack remains, a change from PHEV cells with 180 Wh/kg to a BEV cell with 250 Wh/kg leads to an energy pack density of 130 Wh/kg. The utilization of high energy cells is particularly interesting because the increasing amount of BEVs leads to scaling effects and therefore cost reductions in the battery cell production. The recuperation power $P_{EM,Gen}$ is higher than the propulsion power $P_{EM,Mot}$ for the electrified vehicles to consider the increasing power availability of the EM due to the voltage increase during recuperation. The conventional vehicle compensates the electrical system load with an alternator, which does not provide motoric power. The system load increases with a higher degree of hybridization due to the additional control units as well as higher thermal management requirements. As no heating and air condition model is utilized, the system load is chosen high enough to represent the required annual average power [32].

Table 3. Electric powertrain parameters for different degrees of hybridization.

Property	Symbol	Conv.	48 V HEV	48 V PHEV	HV PHEV
Electric powertrain weight (kg)	$m_{0,Edr}$	0	36	50	50
Battery energy density (Wh/kg)	ρ_{Bat}	0	55	130	95
Maximum motoric power (kW)	$P_{EM,Mot}$	0	20	20	100
Maximum generator power (kW)	$P_{EM,Gen}$	3	25	25	120
12 V electrical system load (W)	P_{Pnt}	700	750	800	800
Combined EM/Inverter efficiency	η_{Edr}	0.7	0.9	0.9	0.9
Converter efficiency	$\eta_{DC/DC}$	1.00	0.95	0.95	0.95
Charge efficiency	η_{Chg}	-	-	0.85	0.85
Battery upper SOC limit	SOC_{Max}	-	0.80	0.95	0.95
Battery lower SOC limit	SOC_{Min}	-	0.3	0.2	0.2

The propulsion power at the transmission input can be split up between the EM and the internal combustion engine (ICE) for the three hybrid types. During propulsion the power demands are defined as

$$P_{EM} = \frac{P_{Whl}}{\eta_{Tra}} \psi_{split} \quad (6)$$

$$P_{ICE} = \frac{P_{Whl}}{\eta_{Tra}} (1 - \psi_{split}) \quad (7)$$

$$-1 \leq \psi_{split} \leq 1 \quad (8)$$

where P_{EM} is the EM power, P_{ICE} is the ICE power, and ψ_{split} is the power split between the EM and ICE. The engine used for this study was a 90 kW turbocharged gasoline engine with direct injection. The efficiency map with the maximum torque and power curve is shown in Figure 5. Temperature effects were not considered in this study.

The electric energy consumption for propulsion is calculated as

$$P_{Bat} = \frac{P_{EM}}{\eta_{Edr}} + \frac{P_{Pnt}}{\eta_{DC/DC}} \quad (9)$$

where P_{Bat} is the battery terminal power, P_{Pnt} is the 12 V electrical system load, and $\eta_{DC/DC}$ is the converter efficiency between 12 V and 48 V or HV. Charging losses for the PHEV systems are considered with the charging efficiency η_{Chg} and are included in the electric energy consumption values.

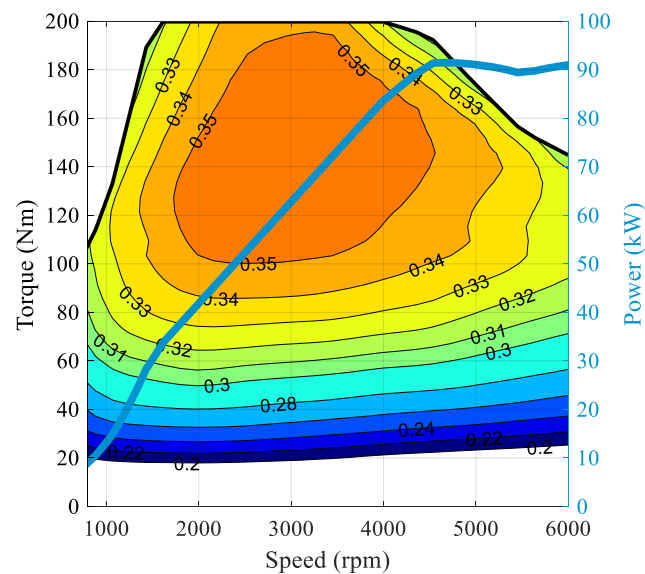


Figure 5. ICE efficiency map, maximum torque (black), and maximum power (blue).

2.3. Battery Pack Modeling

In this study, the battery cells were modeled with measured internal resistance curves. The open-circuit voltage (OCV) and direct current (DC) resistance curves, extracted after a pulse length of five seconds, are shown in Figure 6. Note that the resistance values are normalized by the cell capacity. The high-power 18 Ah 48 V HEV cell showed the lowest internal resistance, whereas the 108 Ah 48 V PHEV cell is a high-energy cell for BEV applications with the highest resistance. The 42 Ah HV PHEV cell has balanced characteristics, so the power-to-energy ratio and internal resistance is located between the other curves. Only discrete battery pack capacities can be configured when the investigated nickel manganese cobalt oxide cells are connected in series or parallel. To comply with the voltage limits and stay in reasonable voltage ranges for the inverter, the number of serial cells was fixed to 12 cells for the 48 V systems and 96 for the HV system. The number of parallel cells varied during the optimization, and was chosen so that the discrete pack capacity matched the required one as closely as possible. For the remaining difference, the cell was scaled to various, continuous capacities

$$C_{Cell} = \delta C_{Cell,measured} \quad (10)$$

where C_{Cell} is the scaled battery cell capacity, δ is the scaling factor, and $C_{Cell,measured}$ is the measured battery capacity. The cell resistance is expressed as

$$R_{Cell} = \frac{R_{i,5s}}{\delta C_{Cell,measured}} \quad (11)$$

where R_{Cell} is the scaled battery cell resistance, and $R_{i,5s}$ is the normalized cell resistance. The pack resistance is then calculated by

$$R_{Pack} = R_{Cell} \frac{n_{ser}}{n_{par}} \quad (12)$$

where n_{ser} is the number of serial cells, and n_{par} is the number of parallel cells.

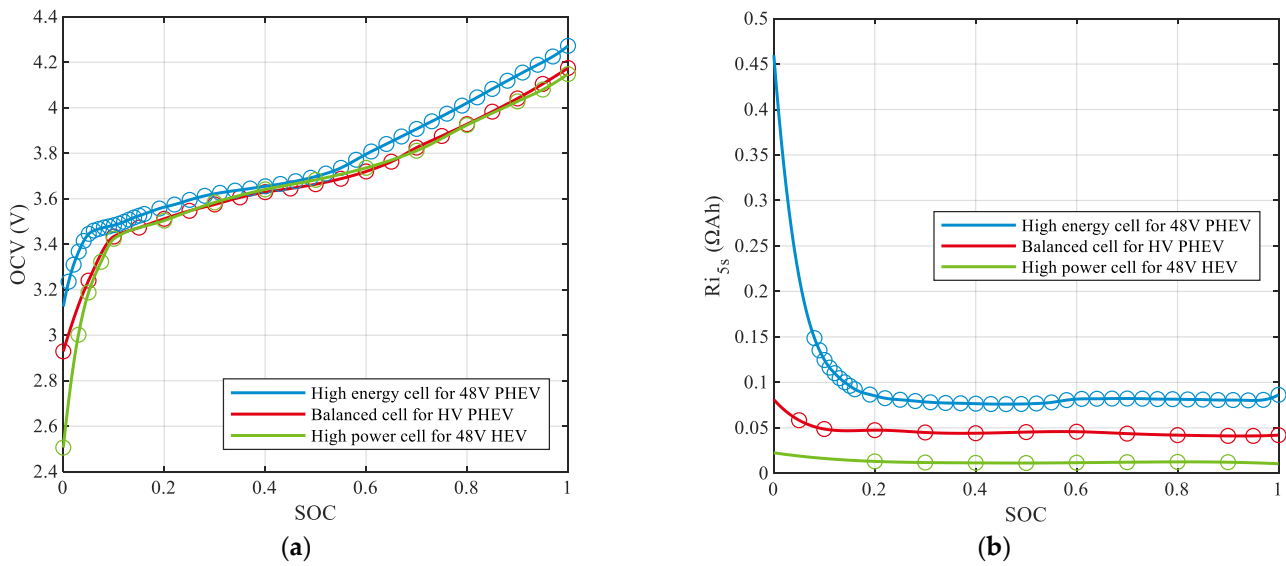


Figure 6. Measured (a) open-circuit voltage and (b) internal resistance curves for three different cell types.

2.4. Energy Management Strategies

The optimal sizing problem is closely related to the EMSs. In literature, Dynamic Programming (DP) [33,34] and ECMS [35,36] are commonly used strategies for powertrain simulations. The former is based on Bellman's principle of optimality [37] and often used as a benchmark solution, as it indicates the optimal fuel consumption if the cycle is known beforehand. A MATLAB function is presented in [38]. The cost function can be written as

$$J = \sum_{t=0}^{N-1} L(x(t), u(t)) \quad (13)$$

where J is the total fuel consumption, L is the fuel consumption matrix, and N is the number of steps in the driving cycle. The costs vary with the state vector $x(t)$, the state of charge (SOC) in this case, and the control input $u(t)$. The control variable determines the engine state and power split between the drivetrain components. $x(t)$ and $u(t)$ are discretized into discrete grids and evaluated during the backward calculation for each time step. The cost-to-go matrix for one timestep can be written as

$$J_t^*(x(t)) = \min_{u(t)} [L(x(t), u(t)) + J_{t+1}^*(x(t+1))] \quad (14)$$

when the initial and final states are defined, all optimal control paths can be found by the algorithm with the lowest possible fuel consumption for this cycle. Implemented constraints for the driveline components ensure the operation within the physical limits.

However, we recognized the influence of a nonoptimal but real-life implementable strategy and compared the DP results to an A-ECMS. The equivalent fuel consumption was calculated as

$$\dot{m}_{f,eq}(\psi_{split}, t) = \dot{m}_{fuel}(\psi_{split}) + s(t) \frac{P_{Bat}(\psi_{split})}{Q_{LHV}} \quad (15)$$

where $\dot{m}_{f,eq}(\psi_{split}, t)$ is the equivalent fuel consumption rate, \dot{m}_{fuel} is the ICE fuel consumption rate, $s(t)$ is the s-factor, and Q_{LHV} is the lower heating value of the fuel. The

torque split was chosen according to the minimal $\dot{m}_{f,eq}(\psi_{split}, t)$ in each time step. The s-factor is controlled by a P-controller

$$s(t) = s_0 + K_p(SOC(t) - SOC_{Target}) \quad (16)$$

where s_0 is the initial s-factor, K_p is the proportional gain, $SOC(t)$ is the current SOC and SOC_{Target} is the target SOC. HEVs drive in charge-sustaining mode (CS), meaning the SOC at the end of the cycle is the same as the starting SOC. Therefore, SOC_{Target} is the starting SOC at $SOC(t_0)$. The two PHEV systems are operated in a CD at the beginning of the cycle until the battery reaches SOC_{Min} . Afterwards, the operating mode switches to a CS mode, where the SOC fluctuates around the lower limit in a narrow range. Accordingly, the target SOC is SOC_{Min} .

To prevent frequent ICE starts in a short amount of time, the minimum ICE runtime was implemented as five seconds in the A-ECMSs. For the first start, the minimum runtime was increased to three minutes to heat up the ICE and exhaust gas treatment.

2.5. Life Cycle Variables

To evaluate the LCA emissions, it would be inaccurate to consider the fossil fuel consumption only. PHEVs in electric mode and BEVs have no tailpipe emissions, but the generation of electric energy produces GHG emissions that influence the LCA results significantly [39]. Additionally, the larger battery contributes to the total vehicle lifetime emissions due to the energy-intensive production.

This study considers the CO₂-equivalent emissions of the production and use-phase of a vehicle. Environmental impacts of the recycling phase for the vehicle and battery are included in the production values coming from other LCA studies. The emissions for the production phase are normalized by km with an assumed vehicle lifetime of 225,000 km. The assumptions are summarized in Table 4.

Table 4. LCA emissions for the production phase and energy sources.

	2020	2030
Conv./48 V HEV production (t CO _{2,eq} /t _{vehicle})	5.20	4.42
PHEV production (t CO _{2,eq} /t _{vehicle})	5.70	4.85
Battery production (kg CO _{2,eq} /kWh)	90	35
Gasoline (g CO _{2,eq} /MJ)	90.4	90.4
Electric energy (g CO _{2,eq} /kWh)	438	254

A weight-based approach from [40] was used to simulate the vehicle production emissions. In our study, the LCA emissions for the production and recycling of the glider and the powertrain from [41] were divided by the average mass of lower medium cars in Europe. For a conventional vehicle, 5.2 t CO_{2,eq}/t_{vehicle} were emitted in 2020, which is assumed to be the same for the 48 V HEV. A PHEV produces slightly more GHG gases, with 5.7 t CO_{2,eq}/t_{vehicle} excluding the battery. The value is expected to decrease by 15% towards 2030 [40]. Emissions for the battery production have changed in recent studies due to more available production data, production plant location shifts, and different chemical compositions. With further improvements, the value is expected to decrease from 90 kg CO_{2,eq}/kWh in 2020 to 35 kg CO_{2,eq}/kWh in 2030 [41], which is a feasible range compared to the extensive literature review in [42].

The emissions of the use-phase include the well-to-tank processes as well. The gasoline emissions are based on a publication of the EU [43] with 90.4 g CO_{2,eq}/MJ, and are expected to remain constant throughout the investigated time horizon. It is important to quantify the year for the GHG emissions of the electric energy, as the electricity mix is moving towards lower emissions due to a higher share of renewable energy sources. In the LCA of the European Commission report [41], the EU 28 CO₂-equivalent emissions for electricity are assumed to be 438 g CO_{2,eq}/kWh for 2020 and 254 g CO_{2,eq}/kWh for 2030. The

assumptions in this study rely on the baseline scenario, which includes all planned or already implemented EU and national policies.

3. Results of Year-Round LCA

In this chapter, the LCA simulation results are discussed. Figure 7 displays the results for a subcompact vehicle and Figure 8 for the compact class vehicle. In the figures, the electric and fuel emission bars represent the A-ECMS simulations. The possible improvements due to an optimal EMS are shown with the white error bars, which indicate the LCA result for the DP results. The optimal battery capacities with the lowest GHG emissions are marked with diamonds; red for the A-ECMS and white for DP. The results for the year 2020 are shown in the top part for each driver; the lower part demonstrates the LCA results for the year 2030. The relative saving potential compared to a conventional vehicle of the corresponding year is given on the right side of each bar. The next subchapters discuss the influence of individual changes on the optimal battery capacity and LCA results.

3.1. EMS Influence

All electrified vehicles were simulated with an A-ECMS and DP, whereas the conventional vehicle only has one result, as the operation strategy has no opportunity to split up the power between different components. The emissions due to the production are not dependent on the EMS, so only the electricity and fuel consumption bars are different. For the 48 V HEV, the GHG reduction potential is solely based on reducing the fuel consumption, as the system does not consume electric energy as a PHEV does. For the PHEVs, the DP-saving potentials can originate from a lower electricity or fuel consumption. However, the emissions due to electricity consumption are only 0.4% smaller on average for a DP subcompact class PHEV compared to the ECMS variant, so the main factor for overall lower GHG is the reduction of the consumed fuel as well.

The reduction potential of the DP relies on three effects. In contrast to DP, the A-ECMS includes parameters that prevent switching the ICE on and off frequently and ensure a minimum runtime. The runtime for heating up the engine has a significant influence on short trips. Secondly, the DP propels the vehicle with a higher efficiency because the cycle is known beforehand and adjusts the SOC accordingly. Finally, the battery is discharged slowly if the cycle length exceeds the electric range for PHEVs. If the electric energy could be used more efficiently at the end of a long trip, the A-ECMS might have already depleted the battery charge.

The benefit of an optimal EMS is the greatest for the 48 V HEV, where it is 5.6% on average for the subcompact vehicle and 5.3% for the compact class vehicle. It shrinks with larger battery capacities and HV systems. If a cycle is shorter than the electric range of the vehicle, it can be completed in pure electric mode, and the two EMS deliver the same result. As this occurs more often for higher battery capacities and an HV system, the difference shrinks between the two EMSs.

The previously mentioned points also affect the optimal battery size, indicated by the red and white diamonds. The optimal battery capacity for a DP-controlled vehicle is slightly smaller for all systems and drivers compared to the ECMS minimum. The optimal EMS propels the vehicle with a higher efficiency, especially at lower capacities, so a larger energy storage is not useful. In some cases, the optimal capacity is outside the range of typical capacities below 30 kWh. In those cases, the results for 30 kWh are extracted, because a further capacity increase would reflect a heavy and expensive BEV with dual powertrains. The values for the optimal battery capacity and corresponding LCA emissions can be observed in Table 5.

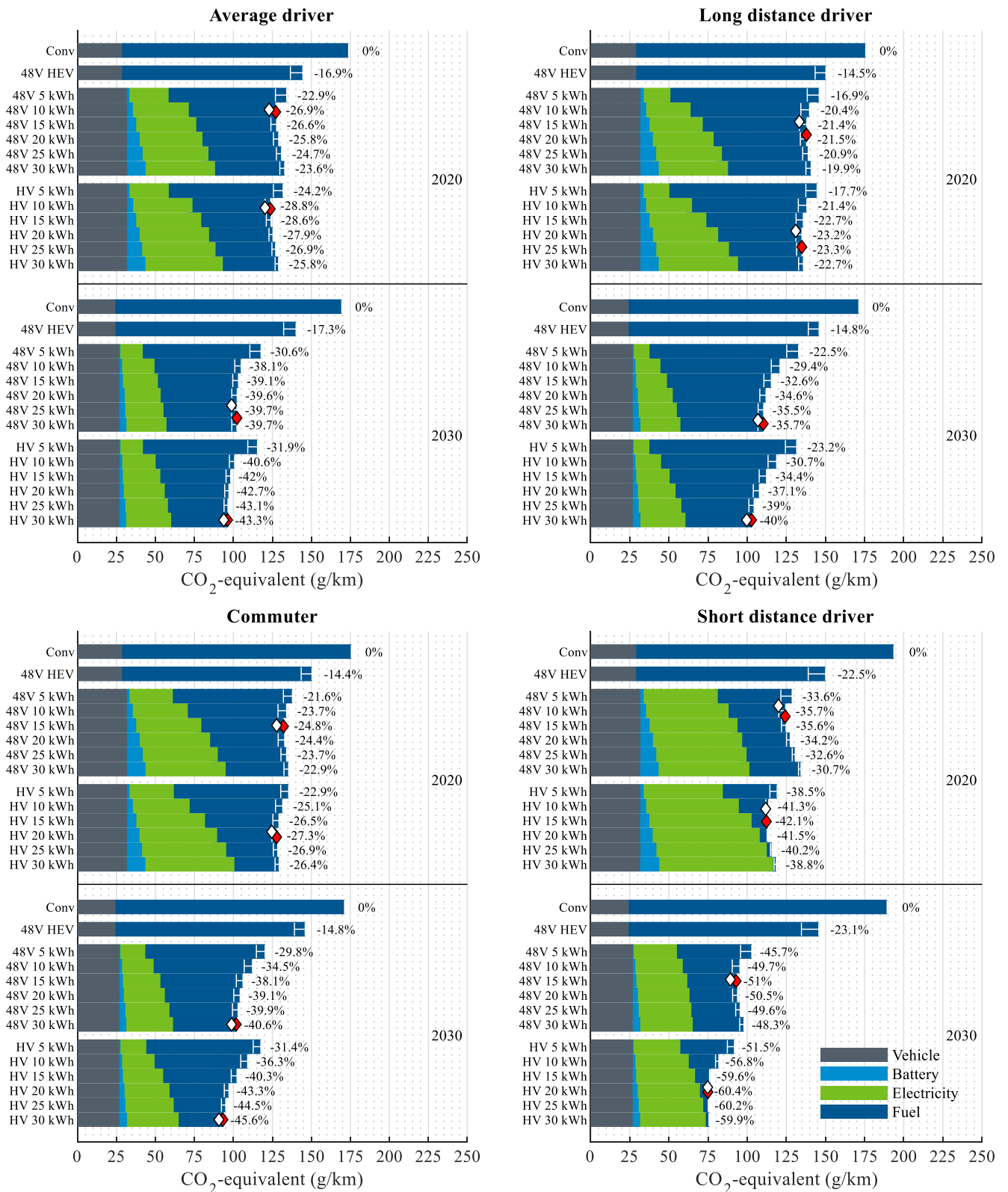


Figure 7. Use case LCA emissions for the subcompact vehicle and ECMS. The colors indicate the emission sources. The white error bars show EMSs optimization potentials with DP. The diamonds mark the minimum LCA systems for ECMS (red) and DP (white).

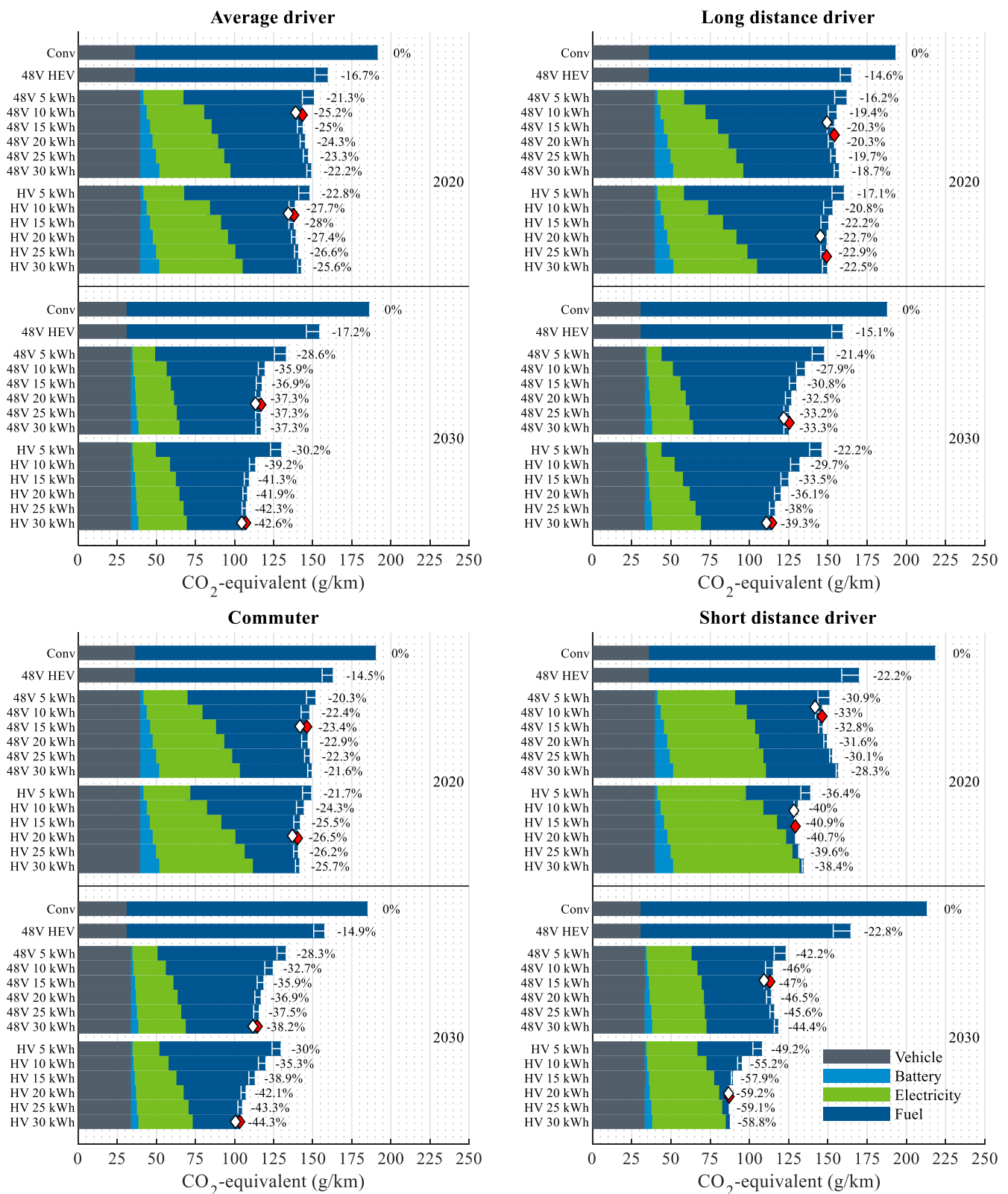


Figure 8. Use case LCA emissions for the compact vehicle and ECMS. The colors indicate the emission sources. The white error bars show EMSs optimization potentials with DP. The diamonds mark the minimum LCA systems for ECMS (red) and DP (white).

Table 5. Derived optimal battery capacities and resulting life cycle GHG emissions.

System		48 V PHEV				HV PHEV				
Year		2020		2030		2020		2030		
EMS		DP	ECMS	DP	ECMS	DP	ECMS	DP	ECMS	
Subcompact class	Capacity (kWh)	Short-distance driver	8.3	12.0	14.6	15.2	11.0	15.3	18.9	20.5
		Average driver	10.0	10.8	23.5	27.8	10.9	11.3	30.0	30.0
		Long-distance driver	14.1	18.5	28.5	29.8	18.8	24.3	30.0	30.0
		Commuter	15.0	15.3	30.0	30.0	18.9	20.7	30.0	30.0
	GHG (gCO _{2,eq} /km)	Short-distance driver	120	124	89	93	112	112	75	75
		Average driver	123	127	99	102	120	124	94	96
		Long-distance driver	133	138	107	110	131	135	100	103
		Commuter	128	132	99	102	125	128	91	93
		Short-distance driver	8.3	11.4	14.3	14.7	11.1	16.5	20.3	21.4
		Average driver	10.2	11.0	22.0	22.3	12.0	12.6	30.0	30.0
Compact class	Capacity (kWh)	Long-distance driver	13.6	17.9	26.9	28.5	19.8	26.7	30.0	30.0
		Commuter	14.9	15.0	30.0	30.0	19.7	20.5	30.0	30.0
		Short-distance driver	142	146	109	113	128	129	87	87
		Average driver	139	143	113	117	134	138	105	107
	GHG (gCO _{2,eq} /km)	Long-distance driver	149	154	122	125	145	149	111	114
		Commuter	142	146	112	115	137	140	101	103

3.2. Influence of Investigated Year

The GHG emissions for the conventional and 48 V HEV systems were reduced overall due to the lower vehicle production emissions, but remained constant in the usage phase throughout the years. As the emissions from the vehicle, battery, and electric energy production decreases in the 2030 scenario, the overall life cycle GHG impact for PHEVs drops significantly in future years. The emissions during the production of the battery have an especially minor influence on the total LCA emissions for PHEVs beyond 2030.

The change of LCA emissions throughout the years depends on the electric driving share because the fuel emissions remain constant. The lowest share of electric driving can be noted for the compact class long-distance driver and a 48 V 5 kWh battery. The relative reduction potential of 16.2% increases to 21.4% in 2030. In contrast to this, the relative potential of 38.4% for the short-distance driver with the largest HV battery, where almost every daily distance can be completed in pure electric mode, increases to 58.8%. Similar values can be seen for the subcompact class.

3.3. Use Case Influence

Four typical driving use cases were defined in Chapter 3 which show a different GHG reduction potential. The baseline emissions for the conventional vehicle are almost the same, except for the short-distance driver. Taking the compact class vehicle as an example, the GHG emissions for the average, long-distance, and commuter driver are between 191 gCO_{2,eq}/km and 194 gCO_{2,eq}/km in 2020. The short-distance driver results in 219 gCO_{2,eq}/km. As the driving style is slightly more aggressive and no start–stop is possible during the heating time, the fuel consumption is higher during short trips. The opposite behavior can be seen for the 48 V HEV, where the relative reduction potential is the largest for the short-distance driver in both vehicle classes. In short trips, the share of mechanical energy for acceleration is higher compared to the rolling, climbing, and air resistance parts. Similarly, the share of recuperation energy is higher compared to the total trip deceleration energy due to the frequent speed changes for the short-distance driver. Consequently, the advantage of a 48 V HEV is very large during short distance trips and decreases with higher trip lengths, which usually have a higher mean speed and are less dynamic.

The results of the LCA for the PHEVs correspond to the statistical driving behavior in the UF curves. The largest relative fuel-saving potential can be achieved by the short-distance driver and the lowest by the long-distance driver. The higher share of electric

driving even overcompensates the higher baseline value of the short-distance conventional vehicle so that the absolute GHG emissions are lower for most of the systems.

The commuter shows no large leap at a certain battery capacity, even though many trips are in a specific distance range. Typical of a work commute, 67% of the trips are within a range of 25 and 45 km. Combined with shorter trips, 76% of the trips have a distance below 45 km and could be completed in mostly pure electric mode with a battery capacity of less than 10 kWh, even for the compact class vehicle. Nevertheless, in 2030, the optimal battery capacity exceeds 30 kWh, although this capacity would electrify 90% of the trips purely. The remaining 10% of the trips are in a range of 210 and 270 km, where battery capacities larger than 30 kWh still reduce the GHG emissions. This is partly due to the assumption that the vehicle is not charged intermediately during the day. A recharge of the battery during long trips would be possible and lead to lower optimal capacities. Nonetheless, this example demonstrates that it is important to consider the trip length, which cannot be driven in charge-depleting mode, and not only the number of trips.

3.4. Vehicle Class Influence

The overall GHG emissions increase for all systems and drivers towards the compact class vehicle because the additional weight has a larger influence on the required wheel energy compared to the slightly lower drag resistance. Furthermore, vehicle production emissions increase due to the additional weight.

The relative potential for the 48 V HEV only varies within 0.3 percentage points between the two classes. This value is larger for the PHEV variants, where the difference can be up to 4 percentage points less for the compact class vehicle. The emissions due to electric energy consumption increase only slightly towards the compact class vehicle because the power demand on wheel level increases. The amount of fuel emissions increases proportionally more, because in addition to the increasing power demand, the electric range decreases, so the vehicle is driven in CS mode more often. For the 48 V PHEV, a higher difference is noticeable because more operating points exceed the power limits of the EM and the number of ICE starts increases.

4. Discussion

4.1. Road towards Climate Neutrality and Potential of 48 V PHEVs

The transport sector needs to achieve lower GHG emissions in the coming years to keep global warming below 1.5 °C. Current regulations within the EU limit the tailpipe emissions and do not consider the whole life cycle of the vehicle. Therefore, a direct comparison between regulatory fleet target limits and the LCA simulation results for individual vehicles is not possible. However, the overarching climate goals are summarized in the European Green Deal, which aims at climate neutrality until 2050 and a GHG reduction of 55% by 2030 compared to 1990. As emissions have already dropped by 24% until 2019 [44], a further reduction of 41% from a 2019 baseline is necessary.

In the current phase of transformation towards electrification, the concept of HEV respective to PHEV has to be regarded as a supplement to BEVs. Hybrids can typically cover those use cases which can't be managed by battery electric vehicles because of, e.g., range limitations, infrastructure, or power requirements. Considering the relatively low costs of a 48 V HEV system, these systems offer an easily implemented solution with a comparably large saving potential and no need for charging infrastructure. The small batteries do not increase the emissions in the production phase significantly, and only a small quantity of additional resources would be necessary. Within a fleet mix, the 48 V PHEV in combination with BEV and other hybrids can significantly contribute to a reduction of GHG emissions and reach future emission targets. Even when incorporating future climate protection efforts, PHEV concepts with their 2030 LCA potential can reduce the overall emissions of the transport sector.

PHEVs rely on frequent charging to electrify as many kilometers as possible. Due to the high daily distances of the long-distance driver, the CD share is smaller, indicated by

the lowest share of electricity emissions. Consequently, the improvements in electricity production have a smaller impact compared to the other drivers. Still, a GHG reduction of at least one-third in 2030 is possible when the vehicle is equipped with a 20 kWh battery. For any upcoming fleet emission scenario, PHEVs are vital to achieve the objectives in 2030 on an LCA data basis. Even small battery capacities help to reduce the overall LCA emissions significantly, but larger capacities compared to today's market average can increase the relative GHG savings. In contrast to the results for 2020, the battery should be as large as possible for the lowest LCA emissions in 2030. Only the short-distance driver has an optimal battery capacity below 30 kWh, but with a negligibly small difference in overall GHG emissions.

As expected, the 48 V PHEV cannot reach the same GHG-saving potentials as an HV PHEV. It still has a large benefit compared to an HEV system, and the overall LCA emissions are similar to the HV vehicle emissions for all use cases and vehicle classes. While HV PHEVs can cover trip distances below the electric distance in pure electric mode, the 48 V PHEV needs to turn on the ICE if the power demand exceeds the limits of the less powerful EM. On the contrary, during very long daily driving distances, the fuel consumption of the 48 V PHEV is lower than the HV PHEV. A large share of the possible recuperation energy can be covered by the 48 V EM and the lower weight results in lower energy demand on wheel level. As these long trips have a higher influence on the year-round fuel consumption, the 48 V PHEV can compensate parts of the higher fuel consumption in short trips. This can be validated in the figures by comparing the relative reduction potential between the 48 V and HV PHEV at different capacities. With 5 kWh, many trips exceed the electric range and the 48 V PHEV results are therefore close to the HV values. With increasing battery capacities, the difference between the two system voltage levels increases.

In addition to CO₂ targets, the 48 V PHEV technology can also be expected to be beneficial with respect to real-driving emissions. The additional battery capacity compared to HEVs offers an increased electric driving share at the start of the vehicle when the exhaust gas aftertreatment system is not conditioned. At the same time, electric catalyst heaters for 48 V systems can be required to meet future emission regulations. Catalyst heaters can ensure the required temperature before the ICE is started. As the ICE is started more frequently compared to HV PHEVs, the average catalyst temperature can be expected to remain at a higher level. This can reduce the additional heating and therefore electric energy demand if the EMS is required to switch on the ICE.

The lower additional powertrain costs for 48 V PHEVs could help to increase the PHEV share in the cost-driven subcompact class market. Substituting more conventional and HEV vehicles with PHEVs reduces the life cycle GHG emissions while the vehicle range remains constant due to the CS phase. Especially in inner-city traffic, where the distances and power requirements are typically low, the ability to drive electrically results in high emission reduction potentials. The lack of HV components also reduces the maintenance and safety issues, which requires specially trained personnel and tools in workshops. On the contrary, electric driving is only possible with limited power, which leads to limited driving dynamics towards heavier vehicle classes. Additionally, the GHG emission-saving potential relies on regular charging of the vehicle.

Although we focused on the European market in this study, other markets around the world are attractive for a 48 V PHEV system as well. Especially in Asian countries, megacities struggle with a dense traffic volume and thus emission issues. At the same time, the traffic jams lead to slow vehicle speeds and therefore low power requirements. In combination with low average vehicle weight, such as in India, large trip shares can be electrified with a 48 V PHEV at a cost-attractive level.

4.2. External Influencing Factors

The results of this study show that next to the dimensioning, several external factors influence the resulting GHG emissions of PHEVs as well. All implications can be applied to 48 V and HV PHEVs in the same manner as the influences have been shown to be

similar. First, the analysis of the real driving behavior showed that only the short-distance driver UF curve is located above the EU WLTP curve. Since the average annual driving distances in the European fleet are in the range of the average driver, the CD shares of most customers are below the estimated shares by the current European UF curve. Though we only compared four drivers to the regulation curve, other studies with larger driving trip databases have shown similar results [45,46]. This issue is crucial for trust in the ability of PHEVs to contribute to the climate goals because the fuel consumption values of the customers diverged from the certified values. However, this study demonstrates that significant fuel consumption and GHG savings are possible with the plug-in technology if the systems are used under the mentioned assumptions. In the future, all new vehicles in the EU are monitored with the introduction of the on-board fuel consumption monitoring systems under real-life conditions. It is planned to use the gained data in future fuel consumption regulations.

Second, the LCA demonstrates the importance of the emissions due to electric energy consumption. Even with the current electricity mix, life cycle GHG emissions can be reduced with PHEVs, but a further inclusion of renewable energy sources into the grid is necessary to increase the GHG reduction potential. The assessment of life-cycle emissions for passenger cars in future years is very important, and its inclusion in the regulation process would help to reach the climate goals on a comprehensive level. The consideration of electricity production GHG is especially important to evaluate the potential of hybridization because the impact on LCA emissions is larger compared to the differences in the production phase. The additional greenhouse gases of the battery production influence the LCA emissions in the future marginally, so the electricity GHG share is even more dominant. Together with increasing market shares of electricity-consuming BEVs and PHEVs, a low-emission electricity mix is vital for the transportation sector.

Finally, the LCA emissions of PHEVs in future years indicate an optimum at much larger battery capacities than the current market average. Considering the effects of the GHGs of the electricity mix show a decreasing trend during the vehicle lifetime, PHEVs with higher battery capacities can help to reduce the emissions today as well. Shrinking battery prices can even allow larger battery capacities for the same additional costs as today, while improvements in the battery cell itself can reduce the weight and volume of the battery packs at the same time [47]. In addition to larger battery capacities, frequent charging increases the electric driving share and thus reduces the LCA emissions of PHEVs. Convenient access to charging stations, fast charging along highways, and competitive energy prices are therefore essential to electrify more driving shares [48]. Besides, it can be expected that additional savings in fuel consumption are achieved by the next generation of ICEs due to stricter emission regulations. The application of dedicated ICEs, which are optimized for the operation in Hybrid-Powertrains, offers further relevant potential [49].

The presented approach covers many driving trips for different vehicle types and EMSs to give a holistic view on the GHG-saving potential. Nevertheless, the LCA results are depended on the input assumptions, which may vary, especially for the 2030 scenario. The GHG-saving potentials need to be investigated for further regions. Also, temperature effects and emission modelling besides CO₂, which influence the environmental impact of PHEVs, have been neglected in our powertrain simulation model [50,51]. Alongside technical aspects, such as the thermal and degradation behavior of a 48 V PHEV battery, the economic analysis of this system bears further research potential [52].

5. Conclusions

In this study, the environmental impact of different electrified systems was investigated and their potential to contribute to climate goals was analyzed. To ensure a realistic and comprehensive comparison, we utilized real-drive data from different drivers and focused on life cycle GHG emissions.

The LCA results reveal that PHEVs can significantly reduce GHG emissions for passenger cars compared to the conventional and 48 V HEV systems. Since the relative reduction

potential of 48 V HEVs is limited to 23% in our case, vehicles with higher degrees of electrification are necessary to meet future regulatory targets and climate goals. Even 48 V PHEV vehicles with a small 5 kWh battery capacity reduce the greenhouse gas emissions by 16 to 34% for the 2020 assumptions. This value is expected to increase up to 46% in the 2030 scenario. Optimal sizing of the energy storage system can increase the emission saving potential even further. Therefore, the PHEV is one promising vehicle technology on the road toward zero-emission mobility.

The 48 V PHEV shows relative saving potentials close to the HV PHEV values. Considering the lower costs, weight, installation space, safety, service, and manufacturing requirements, this technology could open the PHEV market in low-cost vehicle segments. As the results for the subcompact class and compact class vehicles are similar, the GHG savings can be expected to work for many vehicle types. Next to the technological aspects, boundary conditions need to be fulfilled, nonetheless. Regular charging and an increasing share of renewable energies in the grid are key factors for the reduction of GHG emissions. Further research will investigate the battery requirements of 48 V PHEVs with a focus on the aging behavior and effects of BEV cell utilization in this application.

Author Contributions: Conceptualization, T.F.; formal analysis, T.F.; investigation, T.F.; methodology, T.F. and R.K.; software, T.F. and R.K.; supervision, R.L., J.S. and E.F.; visualization, T.F.; writing—original draft, T.F.; writing—review and editing, R.K., R.L., J.S. and E.F. All authors have read and agreed to the published version of the manuscript.

Funding: This research received no external funding.

Conflicts of Interest: The authors declare no conflict of interest.

Nomenclature and Acronyms

A	Frontal Area (m ²)
a_{pos}	Positive acceleration (m/s ²)
$C_{Cell}/C_{Cell,measured}$	Scaled/measured battery cell capacity (Ah)
c_w	Air resistance coefficient
d_i	Distance of daily trip (m)
E_{Bat}	Battery energy (kWh)
f_R	Tire rolling resistance coefficient
g	Gravitational acceleration (m/s ²)
J	Total fuel consumption (kg)
J_t^*	Optimal cost-to-go function at timestep t (kg/s)
L	Fuel consumption matrix (kg/s)
$\dot{m}_{f,eq}$	Equivalent fuel consumption rate (kg/s)
\dot{m}_{fuel}	Fuel consumption rate (kg/s)
$m_{veh}/m_0/m_{0,Edr}$	Vehicle/vehicle base/electric powertrain without battery mass (kg)
N	Driving cycle steps
n	Total number of trips for one driver
n_{ser}/n_{par}	number of serial/parallel cells
K_p	Proportional gain
$P_{EM,Mot}/P_{EM,Gen}$	Maximum motoric/generator power (kW)
$P_{Pnt}/P_{EM}/P_{ICE}/P_{Bat}$	12 V electrical system/EM/ICE/Battery terminal power (W)
Q_{LHV}	Lower heating value (J/kg)
R_{CD}	Charge-depleting range (m)
R_{Cell}	scaled battery cell resistance (Ω)
$R_{i,5s}$	normalized cell resistance (Ω Ah)
r_{dyn}	Tire radius (m)
$SOC_{Max}/SOC_{Min}/SOC/SOC_{Target}$	Battery upper limit/lower limit/current/target SOC

s	s-factor
s_0	Initial s-factor
u	Control input vector
v	Vehicle speed (m/s)
x	State vector
α	Climbing angle
δ	Scaling factor
$\eta_{Tra}/\eta_{Edr}/\eta_{DC/DC}/\eta_{Chg}$	Gearbox/EM and Inverter/DCDC/charging efficiency
Θ	Equivalent rotational inertia (kgm^2)
ρ_{Air}	Air density (kg/m^3)
ρ_{Bat}	Battery gravimetric energy density (kWh/kg)
ψ_{split}	Power split between the EM and ICE
A-ECMS	Adaptive-Equivalent Consumption Minimization Strategy
BEV	Battery electric vehicle
CD	Charge depleting
CS	Charge sustaining
DC	Direct current
DP	Dynamic Programming
EM	Electric machine
EMS	Energy management strategy
EU	European Union
GHG	Greenhouse gas
HEV	Hybrid electric vehicle
HV	High voltage
ICE	Internal combustion engine
LCA	Life cycle assessment
OCV	Open-circuit voltage
PHEV	Plug-in hybrid electric vehicle
RDE	Real-driving emission
RPA	Relative positive acceleration
SOC	State of charge
UF	Utility factor
WLTP	Worldwide Harmonized Light Vehicles Test Procedure

References

1. European Commission. Communication from the commission to the European Parliament, the European Council, the Council, the European Economic and Social Committee and the Committee of the Regions: The European Green Deal. COM(2019)640. 2019. Available online: <https://www.eumonitor.eu/9353000/1/j9vvik7m1c3gyxp/v14cnhyp1ort> (accessed on 13 January 2022).
2. Conway, G.; Joshi, A.; Leach, F.; García, A.; Senecal, P.K. A review of current and future powertrain technologies and trends in 2020. *Transp. Eng.* **2021**, *5*, 100080. [CrossRef]
3. Ou, S.; Gohlke, D.; Lin, Z. Quantifying the impacts of micro- and mild-hybrid vehicle technologies on fleetwide fuel economy and electrification. *eTransportation* **2020**, *4*, 100058. [CrossRef]
4. Benajes, J.; García, A.; Monsalve-Serrano, J.; Martínez-Boggio, S. Optimization of the parallel and mild hybrid vehicle platforms operating under conventional and advanced combustion modes. *Energy Convers. Manag.* **2019**, *190*, 73–90. [CrossRef]
5. Dahodwala, M.; Joshi, S.; Dhanraj, F.; Ahuja, N.; Koehler, E.; Franke, M.; Tomazic, D. Evaluation of 48V and High Voltage Parallel Hybrid Diesel Powertrain Architectures for Class 6–7 Medium Heavy-Duty Vehicles. *SAE Tech. Pap.* **2021**. [CrossRef]
6. Enang, W.; Bannister, C. Modelling and control of hybrid electric vehicles (A comprehensive review). *Renew. Sustain. Energy Rev.* **2017**, *74*, 1210–1239. [CrossRef]
7. Ali, A.M.; Söffker, D. Towards Optimal Power Management of Hybrid Electric Vehicles in Real-Time: A Review on Methods, Challenges, and State-Of-The-Art Solutions. *Energies* **2018**, *11*, 476. [CrossRef]
8. Hu, X.; Han, J.; Tang, X.; Lin, X. Powertrain Design and Control in Electrified Vehicles: A Critical Review. *IEEE Trans. Transp. Electrification* **2021**, *7*, 1990–2009. [CrossRef]
9. Lauer, S.; Perugini, M.; Weldle, R.; Graf, F. 48 Volt High Power—Much More than a Mild Hybrid. In Proceedings of the 29th Aachen Colloquium Sustainable Mobility 2020, Aachen, Germany, 5–7 October 2020.
10. Oechslen, H.; Binder, T.; Cramme, M.; Warth, M. Flexible 48-V Electrification with an Optimum Cost-benefit Ratio. *ATZ Electron. Worldw.* **2019**, *14*, 30–35. [CrossRef]
11. Fritsch, K.-M.; Rieger, D.; Warth, M.; Scharrer, O. 48-V Drive Module for Electric Vehicles. *MTZ Worldw.* **2018**, *79*, 28–33. [CrossRef]

12. Werra, M.; Küçükay, F. CO₂-Analysis and Dimensioning of 48V Hybrid Drivetrains in Legal and Customer Based Cycles. In Proceedings of the 28th Aachen Colloquium Automobile and Engine Technology 2019, Aachen, Germany, 7–9 October 2019; pp. 1431–1448.
13. Decker, L.; Förster, D.; Gauterin, F.; Doppelbauer, M. Physics-Based and Data-Enhanced Model for Electric Drive Sizing during System Design of Electrified Powertrains. *Vehicles* **2021**, *3*, 31. [[CrossRef](#)]
14. Kapus, P.; Brendel, M.; Teuschl, G.; Pels, T. 48-V Plug-in Hybrid Vehicles for Inner-city Zero Emission. *ATZ Worldw.* **2019**, *121*, 26–33. [[CrossRef](#)]
15. Song, Z.; Zhang, X.; Li, J.; Hofmann, H.; Ouyang, M.; Du, J. Component sizing optimization of plug-in hybrid electric vehicles with the hybrid energy storage system. *Energy* **2018**, *144*, 393–403. [[CrossRef](#)]
16. Huang, Y.; Wang, H.; Khajepour, A.; Li, B.; Ji, J.; Zhao, K.; Hu, C. A review of power management strategies and component sizing methods for hybrid vehicles. *Renew. Sustain. Energy Rev.* **2018**, *96*, 132–144. [[CrossRef](#)]
17. Mahmoodi-k, M.; Montazeri-Gh, M.; Madanipour, V. Simultaneous Multi-Objective Optimization of a PHEV Power Management System and Component Sizing in Real World Traffic Condition. *Energy* **2021**, *233*, 121111. [[CrossRef](#)]
18. Xie, S.; Hu, X.; Zhang, Q.; Lin, X.; Mu, B.; Ji, H. Aging-aware co-optimization of battery size, depth of discharge, and energy management for plug-in hybrid electric vehicles. *J. Power Sources* **2020**, *450*, 227638. [[CrossRef](#)]
19. Du, J.; Zhang, X.; Wang, T.; Song, Z.; Yang, X.; Wang, H.; Ouyang, M.; Wu, X. Battery degradation minimization oriented energy management strategy for plug-in hybrid electric bus with multi-energy storage system. *Energy* **2018**, *165*, 153–163. [[CrossRef](#)]
20. Bansal, S.; Dey, S.; Khanra, M. Energy storage sizing in plug-in Electric Vehicles: Driving cycle uncertainty effect analysis and machine learning based sizing framework. *J. Energy Storage* **2021**, *41*, 102864. [[CrossRef](#)]
21. Shaobo, X.; Qiankun, Z.; Xiaosong, H.; Yonggang, L.; Xianke, L. Battery sizing for plug-in hybrid electric buses considering variable route lengths. *Energy* **2021**, *226*, 120368. [[CrossRef](#)]
22. Zhang, L.; Liu, W.; Qi, B. Energy optimization of multi-mode coupling drive plug-in hybrid electric vehicles based on speed prediction. *Energy* **2020**, *206*, 118126. [[CrossRef](#)]
23. Plötz, P.; Funke, S.A.; Jochem, P.; Wietschel, M. CO₂ Mitigation Potential of Plug-in Hybrid Electric Vehicles larger than expected. *Sci. Rep.* **2017**, *7*, 16493. [[CrossRef](#)]
24. Plötz, P.; Funke, S.A.; Jochem, P. Empirical Fuel Consumption and CO₂ Emissions of Plug-In Hybrid Electric Vehicles. *J. Ind. Ecol.* **2018**, *22*, 773–784. [[CrossRef](#)]
25. Onat, N.C.; Kucukvar, M.; Tatari, O. Conventional, hybrid, plug-in hybrid or electric vehicles? State-based comparative carbon and energy footprint analysis in the United States. *Appl. Energy* **2015**, *150*, 36–49. [[CrossRef](#)]
26. Andersson, Ö.; Börjesson, P. The greenhouse gas emissions of an electrified vehicle combined with renewable fuels: Life cycle assessment and policy implications. *Appl. Energy* **2021**, *289*, 116621. [[CrossRef](#)]
27. KBA. Inländerfahrleistung. Available online: https://www.kba.de/DE/Statistik/Kraftverkehr/VerkehrKilometer/vk_inlaenderfahrleistung/vk_inlaenderfahrleistung_node.html (accessed on 13 January 2022).
28. Xia, H.; Li, T.; Wang, B.; He, P.; Chen, Y. Energy Management Optimization for Plug-In Hybrid Electric Vehicles Based on Real-World Driving Data. *SAE Tech. Pap.* **2019**. [[CrossRef](#)]
29. European Commission. Regulation (EU) 2017/1151 of the European Parliament and of the Council. *Off. J. Eur. Union* **2017**, *175*, 1–643.
30. Hao, X.; Yuan, Y.; Wang, H.; Ouyang, M. Plug-in hybrid electric vehicle utility factor in China cities: Influencing factors, empirical research, and energy and environmental application. *eTransportation* **2021**, *10*, 100138. [[CrossRef](#)]
31. Diaz, S. *European Vehicle Market Statistics Pocketbook 2020/2021*; The International Council on Clean Transportation: San Francisco, CA, USA, 2021.
32. Carlson, R.B.; Wishart, J.; Stutenberg, K. On-Road and Dynamometer Evaluation of Vehicle Auxiliary Loads. *SAE Int. J. Fuels Lubr.* **2016**, *9*, 260–268. [[CrossRef](#)]
33. Tian, Y.; Liu, J.; Yao, Q.; Liu, K. Optimal Control Strategy for Parallel Plug-in Hybrid Electric Vehicles Based on Dynamic Programming. *World Electr. Veh. J.* **2021**, *12*, 85. [[CrossRef](#)]
34. Wang, X.; He, H.; Sun, F.; Zhang, J. Application Study on the Dynamic Programming Algorithm for Energy Management of Plug-in Hybrid Electric Vehicles. *Energies* **2015**, *8*, 3225–3244. [[CrossRef](#)]
35. Cai, Y.; Ouyang, M.G.; Yang, F. Impact of power split configurations on fuel consumption and battery degradation in plug-in hybrid electric city buses. *Appl. Energy* **2017**, *188*, 257–269. [[CrossRef](#)]
36. Zeng, Y.; Cai, Y.; Kou, G.; Gao, W.; Qin, D. Energy Management for Plug-In Hybrid Electric Vehicle Based on Adaptive Simplified-ECMS. *Sustainability* **2018**, *10*, 2060. [[CrossRef](#)]
37. Bellman, R. Dynamic programming. *Science* **1966**, *153*, 34–37. [[CrossRef](#)] [[PubMed](#)]
38. Sundstrom, O.; Guzzella, L. A generic dynamic programming Matlab function. In Proceedings of the 2009 IEEE Control Applications, (CCA) & Intelligent Control, (ISIC), St. Petersburg, Russia, 8–10 July 2009; pp. 1625–1630.
39. Tang, B.; Xu, Y.; Wang, M. Life Cycle Assessment of Battery Electric and Internal Combustion Engine Vehicles Considering the Impact of Electricity Generation Mix: A Case Study in China. *Atmosphere* **2022**, *13*, 252. [[CrossRef](#)]
40. Bieker, G. *A Global Comparison of the Life-Cycle Greenhouse Gas Emissions of Combustion Engine and Electric Passenger Cars*; The International Council on Clean Transportation: San Francisco, CA, USA, 2021.

41. Nikolas, H.; Sofia, A.; Samantha, M.-P.; Tom, N.; Judith, B.; Hinrich, H.; Horst, F.; Kirsten, B.; Nabil, A.; Julius, J.; et al. *Determining the Environmental Impacts of Conventional and Alternatively Fuelled Vehicles through LCA*; Ricardo-AEA, ifeu, and E4tech report for the European Commission; Publications Office of the European Union: Luxembourg, 2020. [[CrossRef](#)]
42. Bouter, A.; Guichet, X. The greenhouse gas emissions of automotive lithium-ion batteries: A statistical review of life cycle assessment studies. *J. Clean. Prod.* **2022**, *344*, 130994. [[CrossRef](#)]
43. Prussi, M.; Yugo, M.; de Prada, L.; Padella, M.; Edwards, R.; Lonza, L. *JEC Well-to-Tank Report v5, EUR 30269 EN*; Publications Office of the European Union: Luxembourg, 2020. [[CrossRef](#)]
44. European Environment Agency. *Trends and Projections in Europe 2021*; EEA Report; Publications Office of the European Union: Luxembourg, 2021.
45. Paffumi, E.; de Gennaro, M.; Martini, G. Alternative utility factor versus the SAE J2841 standard method for PHEV and BEV applications. *Transp. Policy* **2018**, *68*, 80–97. [[CrossRef](#)]
46. Plötz, P.; Moll, C.; Bieker, G.; Mock, P.; Li, Y. *Real-World Usage of Plug-In Hybrid Electric Vehicles: Fuel Consumption, Electric Driving, and CO₂ Emissions*; The International Council on Clean Transportation: San Francisco, CA, USA, 2020.
47. Wu, F.; Maier, J.; Yu, Y. Guidelines and trends for next-generation rechargeable lithium and lithium-ion batteries. *Chem. Soc. Rev.* **2020**, *49*, 1569–1614. [[CrossRef](#)]
48. Mandev, A.; Plötz, P.; Sprei, F. The effect of plug-in hybrid electric vehicle charging on fuel consumption and tail-pipe emissions. *Environ. Res. Commun.* **2021**, *3*, 81001. [[CrossRef](#)]
49. Huin, X.; Di Loreto, M.; Bideaux, E.; Benzaoui, H. Improving performance specifications of internal combustion engine dedicated to plug-in hybrid electric vehicles based on coupled optimization methodology. *Trans. Inst. Meas. Control.* **2021**, *45*, 1–12. [[CrossRef](#)]
50. Jung, H. Fuel Economy of Plug-In Hybrid Electric and Hybrid Electric Vehicles: Effects of Vehicle Weight, Hybridization Ratio and Ambient Temperature. *World Electr. Veh. J.* **2020**, *11*, 31. [[CrossRef](#)]
51. Feinauer, M.; Ehrenberger, S.; Epple, F.; Schripp, T.; Grein, T. Investigating Particulate and Nitrogen Oxides Emissions of a Plug-In Hybrid Electric Vehicle for a Real-World Driving Scenario. *Appl. Sci.* **2022**, *12*, 1404. [[CrossRef](#)]
52. Wróblewski, P.; Kupiec, J.; Drożdż, W.; Lewicki, W.; Jaworski, J. The Economic Aspect of Using Different Plug-In Hybrid Driving Techniques in Urban Conditions. *Energies* **2021**, *14*, 3543. [[CrossRef](#)]